

Exploring European Space Agency Sentinel-2 Satellite Multispectral Band Combinations for Land Use Classification

Prepared by Charles Buniger

Abstract

Terrestrial observations acquired via space borne satellite are invaluable for studying the Earth and its ecosystems. Remotely sensed data makes it possible to visualize, quantify, and analyze the various land cover types in a way that is impossible by other means due to the massive scale on which they occur. The additional temporal component of the information allows for detecting and tracking environmental changes at these large scales. The Sentinel-2 constellation of Multi Spectral Instrument (MSI) satellites was launched on June 23 of 2015 by the European Space Agency (ESA) with the mission to provide publicly-accessible medium-resolution remotely sensed data in support of vegetation, land cover, and environmental monitoring studies.¹ The data provided by the ESA is comparable to both legacy and contemporaneous Landsat imagery managed by the United States Geological Survey (USGS) and should help maintain the continuity of temporal observations. There are however differences in spatial and spectral resolution between the imagery collected and provided by the ESA and USGS. This report seeks to identify these differences and successfully execute a supervised land-use classification upon different band combinations of Sentinel-2 data.

Data description

The Sentinel imagery for this project was acquired through the USGS Earth Explorer portal on November 27th, 2018 and was collected July 1st, 2018. The data consists of 13 radiometric bands and has been processed to Level-1C. This processing level “includes radiometric and geometric corrections including ortho-rectification and spatial registration on a global reference system with sub-pixel accuracy”.² The spatial and spectral characteristics of each band are shown in the figure below.

Sentinel-2 bands	Sentinel-2A		Sentinel-2B		Spatial resolution (m)
	Central wavelength (nm)	Bandwidth (nm)	Central wavelength (nm)	Bandwidth (nm)	
Band 1 – Coastal aerosol	443.9	27	442.3	45	60
Band 2 – Blue	496.6	98	492.1	98	10
Band 3 – Green	560.0	45	559	46	10
Band 4 – Red	664.5	38	665	39	10
Band 5 – Vegetation red edge	703.9	19	703.8	20	20
Band 6 – Vegetation red edge	740.2	18	739.1	18	20
Band 7 – Vegetation red edge	782.5	28	779.7	28	20
Band 8 – NIR	835.1	145	833	133	10
Band 8A – Narrow NIR	864.8	33	864	32	20
Band 9 – Water vapour	945	26	943.2	27	60
Band 10 – SWIR – Cirrus	1373.5	75	1376.9	76	60
Band 11 – SWIR	1613.7	143	1610.4	141	20
Band 12 – SWIR	2202.4	242	2185.7	238	20

Figure 1: Radiometric and spatial resolutions of Sentinel-2 imagery.³

The two instruments that comprise the Sentinel constellation operate at an altitude of 488 miles with sun synchronous orbit, have a push broom configuration, and a five-day revisit time. The images are coded on 12 bits and available in JPEG2000 format with GML header.³ The “USGS Earth Resources Observation and Science (EROS) Center repackages each Sentinel-2 product bundle on a per tile basis, resulting in a file size of approximately 650 Mb. Each Level-1C product is a 100 km x 100 km tile” and are projected into the appropriate Universal Transverse Mercator zone using the WGS 1984 datum. It is also during the L-1C processing step that Top of Atmosphere (TOA) reflectance is calculated.² Key differences between the LandSAT and Sentinel-2 products include: LandSAT has a sixteen-day revisit time, fewer spectral bands (The Sentinel-2 program omits the thermal infrared band⁴), and worse spatial resolution (30m vs. 10m for RGB & NIR).⁵ LandSAT represents the longest continuous collection of satellite data but it would appear that the ESA did a great job of designing their program to complement LandSAT and further the Earth observation sciences.

The area of interest for this project is 15.5 miles wide (East-to-West), 9 miles tall (North-to-South), centered at (38°30'42.72", 107°1'48.19") and encompasses a wide variety of land cover types including the town of Gunnison, Colorado. This area was chosen for its diverse and familiar landcover which should help with choosing classification training pixels as well as reinforce the verification of the of the classification results.

Methods

The imagery used for the following land cover classification was downloaded from the USGS Earth Explorer data portal and unzipped into its native JPEG2000 format. The ESA provides at no cost a very robust piece of software to enable users to view and process remotely sensed data. The STEP software package for Sentinel-2 data was downloaded and installed to facilitate the atmospheric correction of the Sentinel-2 level 1C data to level 2C data. Level 2 processing utilizes level 1C data to convert TOA reflectance to “an orthoimage Bottom-Of-Atmosphere (BOA) corrected reflectance product” that retains the original L1C geometric and radiometric corrections.⁶ The ESA STEP program requires a third-party plugin called “Sen2Cor” to perform this conversion. This plugin was obtained and proved impossible to install and utilize at this time. Strictly speaking, since this project did not have a temporal component, atmospheric correction was not required but the author wanted to further explore the process, so it was decided to utilize the publicly available program QGIS to perform the conversion to a level 2C product. QGIS also uses a third-party plugin called the “Semi-Automatic Classification Tool” to extend its core functionality. The Semi-Automatic Classification tool has specific functions for Sentinel-2 atmospheric correction and is very user friendly. This process takes the top of atmosphere reflectance Digital Number, rescales it by dividing by 10,000, applies coefficients and offsets from the supplied image metadata, and returns an 8-bit .TIF image with values representing reflectance at the bottom of atmosphere.⁵ The original imagery contained no clouds in the area of interest so only haze removal was performed. The resulting bands were then utilized to create composite images with different spectral band combinations that leverage the physical absorption and reflectance properties of the various materials in the area of interest. The five resulting composite images are shown in figures three through seven with brief descriptions of the effect that different band combinations have upon the visual display. The atmospheric correction and image compositing processes described thus far are illustrated in the flowchart shown in figure 2 below. The subsequent image clipping and classification steps are also included in the flowchart and described on page six.

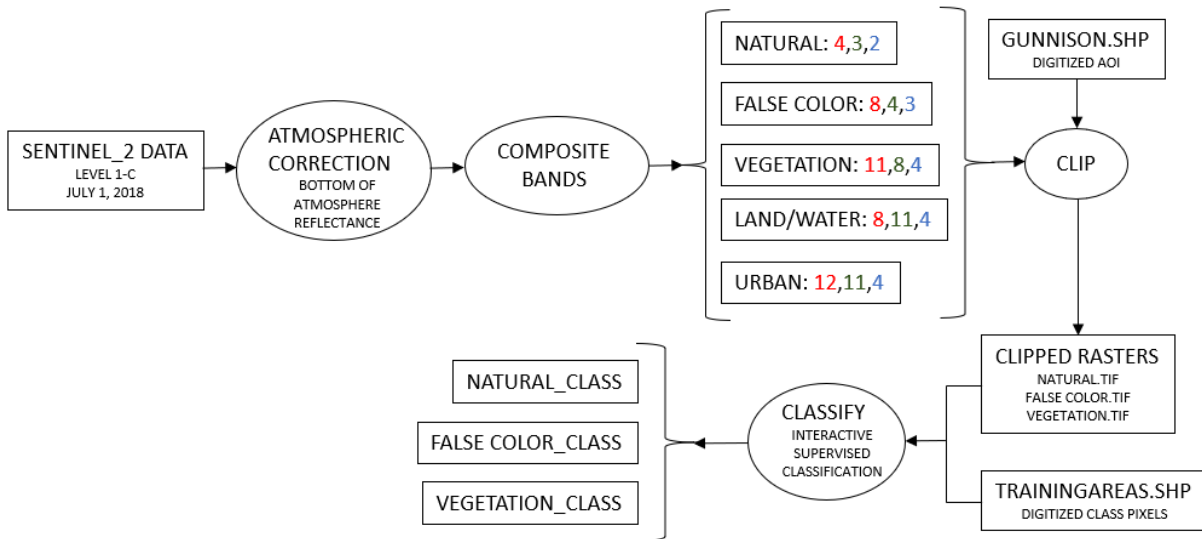


Figure 2: Flowchart illustrating datasets (rectangles) and processes performed (ellipses).

The true natural color band combination shown below is a result the Red, Green, and Blue (RGB) spectral bands detected by the satellite are mapped to the RGB channels of the display. This image best represents the image as our eyes would interpret it but does not enhance any particular land cover type.



Figure 3: Natural Color band combination. Red=B4(Red), Green=B3(Green), Blue=B2(Blue)

The color infrared image shown on the following page draws attention to healthy vegetative land cover by mapping the Near Infrared spectral band to the red display channel. The image “appears this way because vegetation has a high reflectance in the NIR while chlorophyll and water in vegetation have a high absorption of red (displayed as green)”.

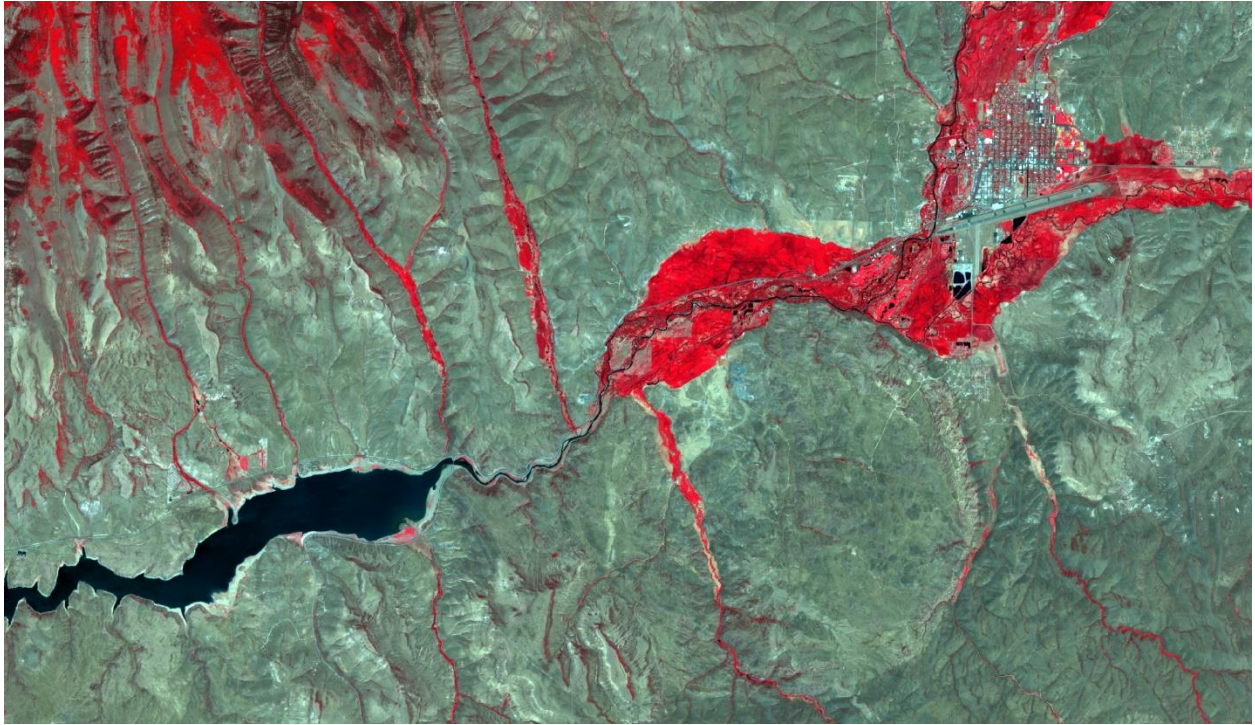


Figure 4: False color infrared image. Red=B8(NIR), Green=B4(Red), Blue= B3(Green)

The image in figure 5 uses both of Sentinel-2's shortwave infrared bands to provide contrast between the natural and manmade components of the landscape. Water is highly absorptive of these bands so it appears very dark.⁷

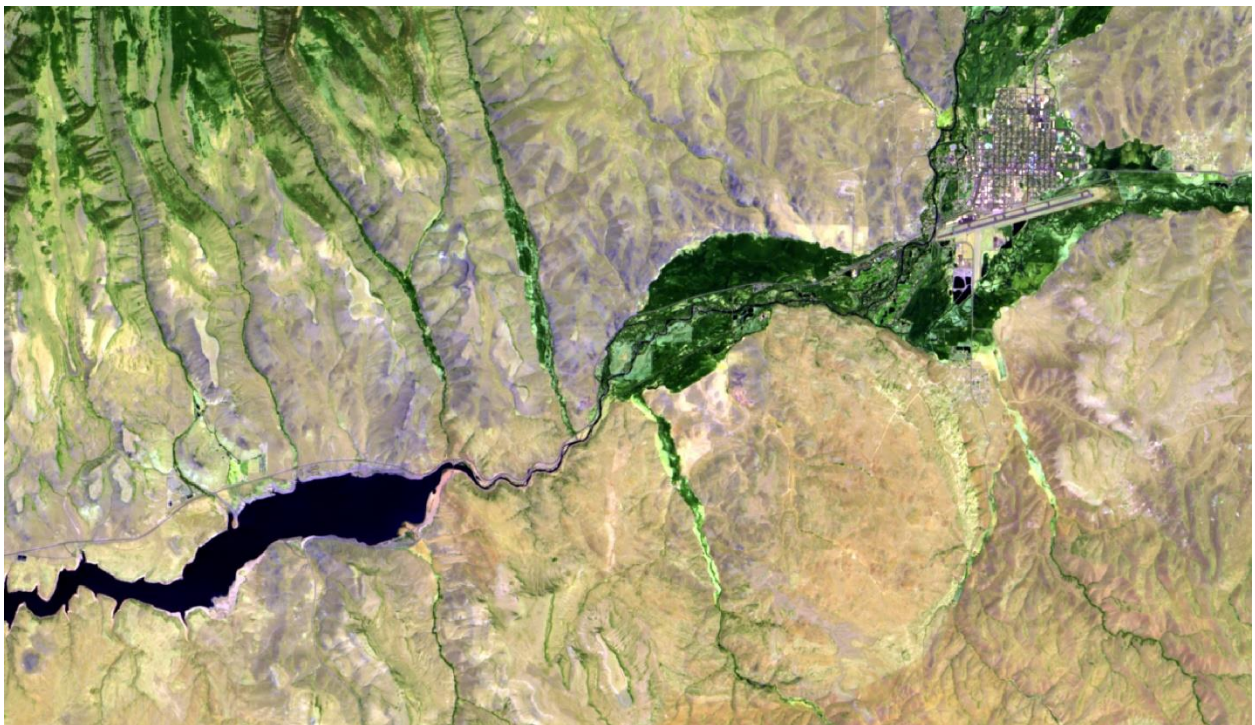


Figure 5: False color infrared highlights urban areas in purple. R=B12(SWIR 2), G=B11(SWIR 1), B=B4(Red)

The images shown below in figures 6 and 7 have the shortwave IR and NIR bands swapped in the red and green display channels. These spectral images do well at penetrating atmospheric particles and haze and are “useful for examining vegetation, coastlines, and other water bodies”.⁷

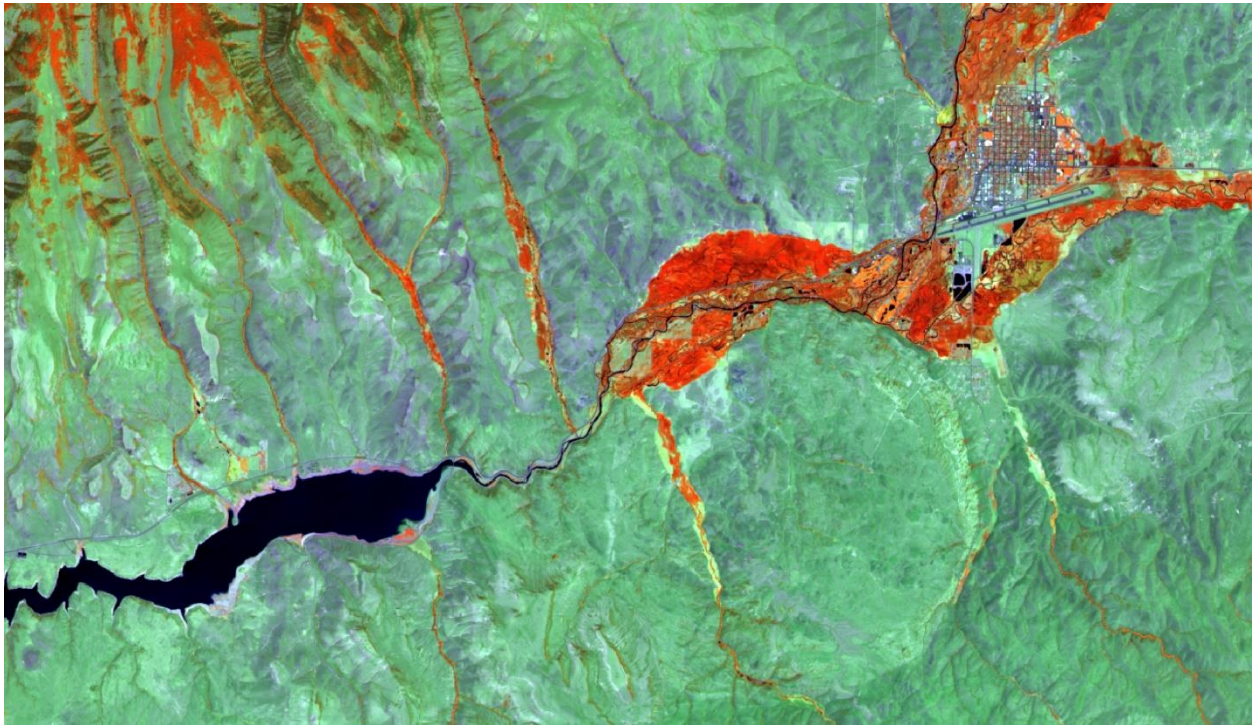


Figure 6: Land/Water Combination. $R=B8(NIR)$, $G=B11(SWIR\ 1)$, $B=B4(Red)$

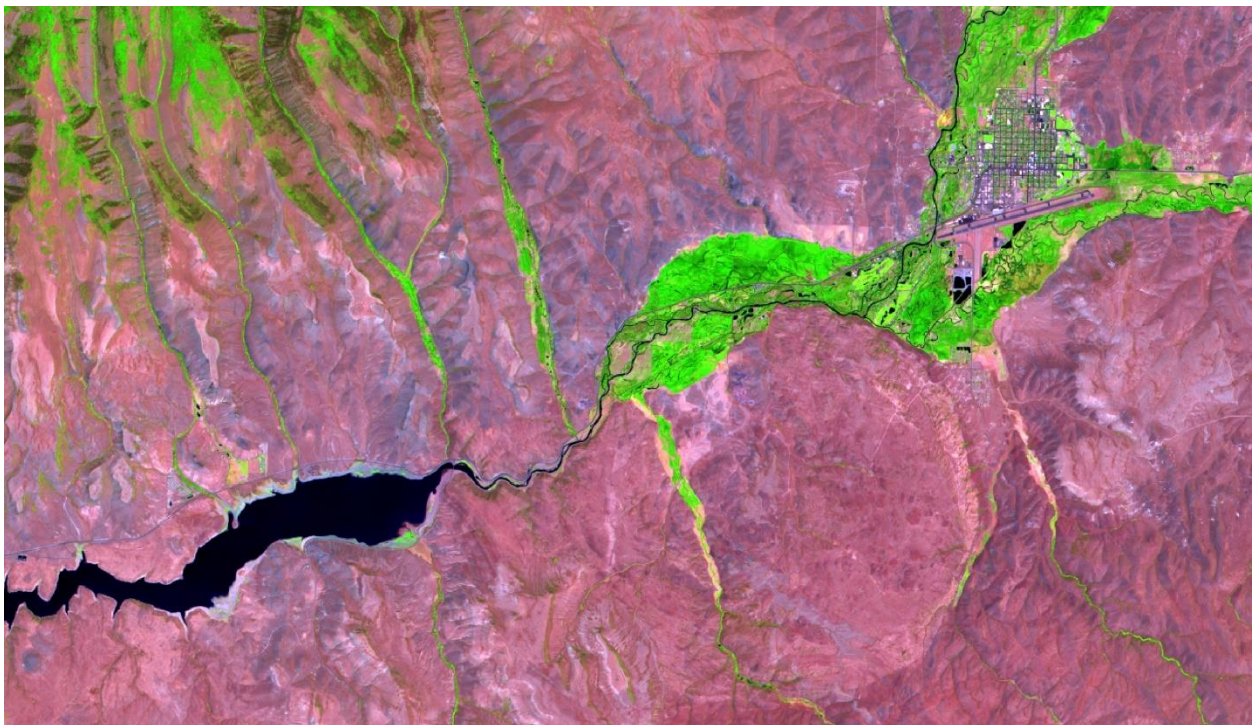


Figure 7: Vegetative band combination. $R=B11(SWIR\ 1)$, $G=B8(NIR)$, $B=B4(Red)$

Determination of the land cover types in the area of interest involved applying a supervised classification to the images. This type of classification technique was originally developed for use with the Landsat Multispectral Scanner (MSS) and requires human guidance. The process involves selecting areas of the image with similar spectral characteristics that will define the class of land cover. The pixels in the image to be classified are then statistically compared to the numeric values of the training area and assigned to the appropriate class.⁸ Therefore the next step was to identify the most homogeneous areas of a particular land cover class in order to generate the purest spectral sample of that particular land cover. These areas are known as the Region of Interest (ROI). The natural color image was used to delineate the ROI's and the result was saved to a separate shapefile with an attribute identifying the type of land cover. Eleven classes were identified based on the authors experience in the area as well as visual interpretation of the image. The legend for the land cover classes is shown in figure eight below.



Figure 8: Legend for land cover classes.

The “Interactive Supervised Classification” tool in ArcGIS was then invoked on the natural color, false color infrared, and vegetative band combination images. This tool utilizes the “maximum likelihood” algorithm to “consider the mean and covariance of the class signature when assigning each cell to one of the classes represented in the signature file. With the assumption that the distribution of a class sample is normal, a class can be characterized by the mean vector and covariance matrix. Given these two characteristics for each cell value, the statistical likelihood is computed for each class to determine the membership of the cells to the class”.⁹ The composite images of different band combinations were then classified using the same ROI's that were manually selected from the natural color composite. The resulting classified images are shown below in figures 9, 10, and 11.

Results

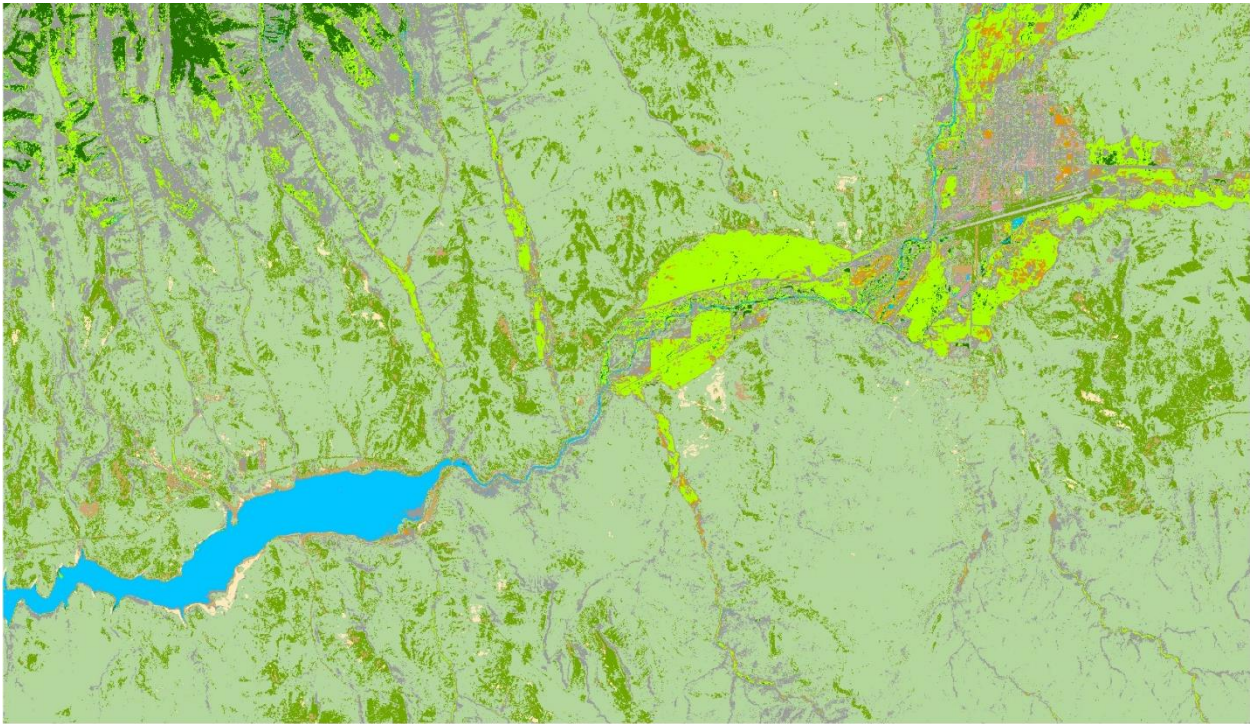


Figure 9: Natural color image classification.

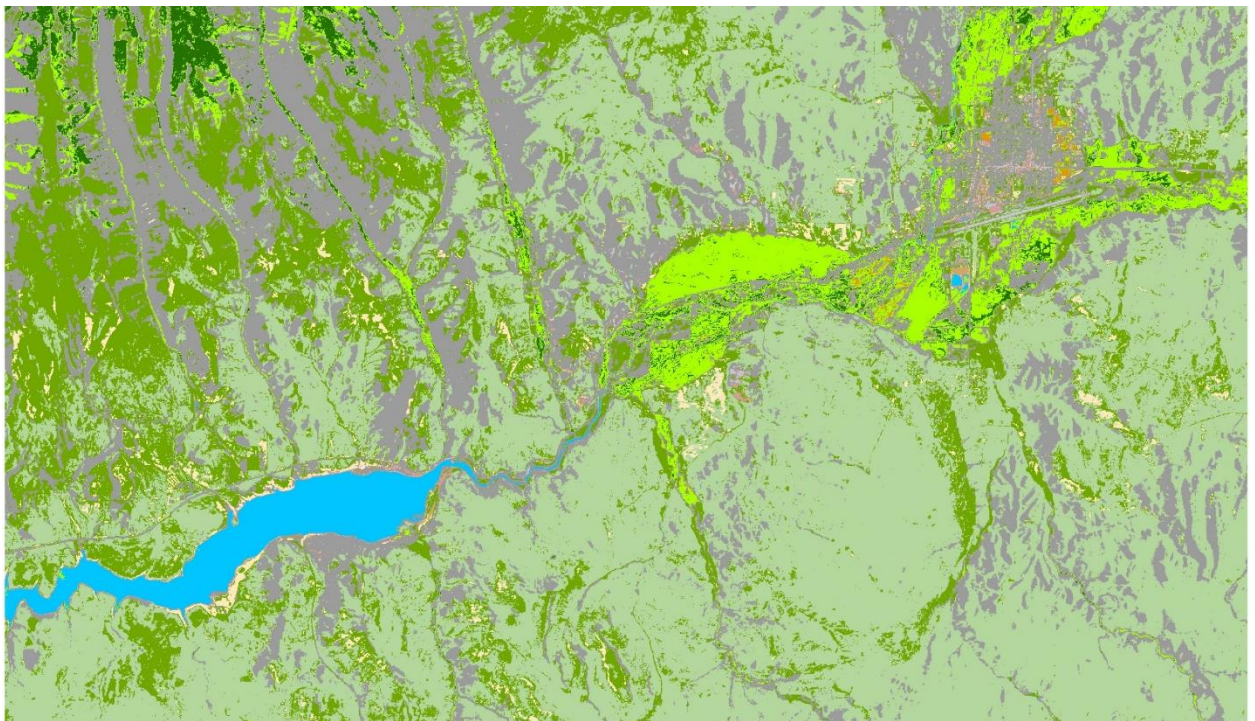


Figure 10: Vegetation band combination classification

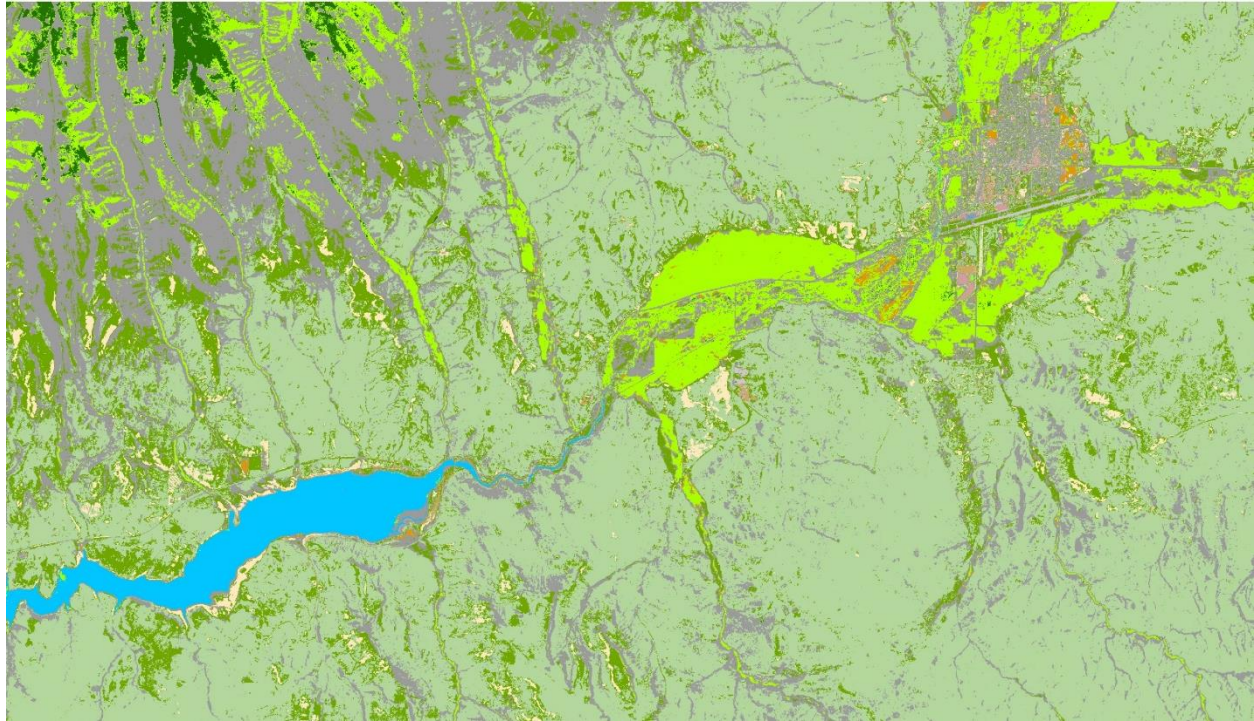


Figure 11: False color band combination classification

The classification process identified eleven different land cover types based on the spectral signature of the selected training areas. The above images appear very similar because the same color scheme was applied to them all. However, examining the areas of each class reveals significant differences in the way pixels were assigned. To assess the accuracy of these classifications a confusion matrix was calculated according to the flowchart shown below. The classified image derived from the same natural color image as the training pixels was used to create the accuracy assessment confusion shapefile containing 100 discrete points. This shapefile was overlaid onto the classifications derived from the false color infrared and vegetation band combination images. The land cover type values were extracted from these images to a new column in the confusion shapefile which then had a confusion matrix calculated from it. These matrices are shown in figures 13 and 14.

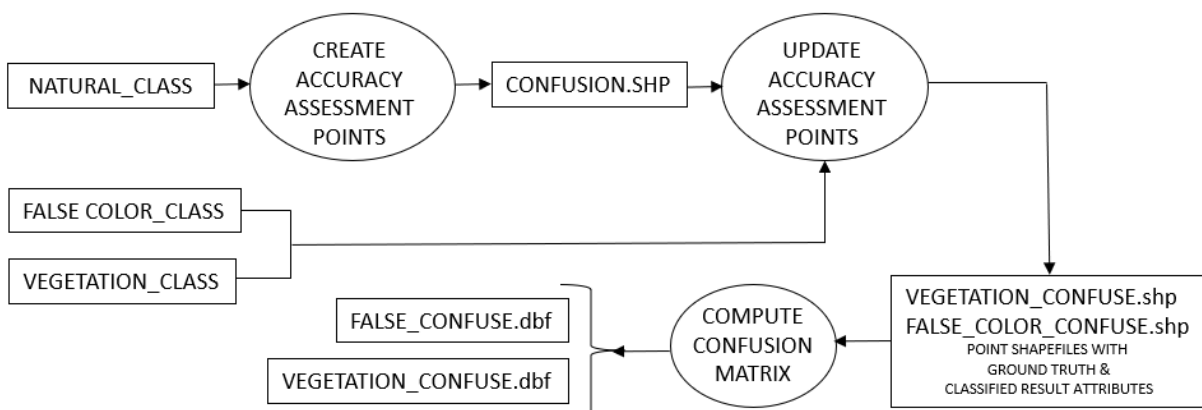


Figure 12: Confusion matrix generation flowchart.

Table

FALSE_CONFUSE

	OID	ClassValue	C_1	C_2	C_3	C_4	C_5	C_10	C_11	C_12	C_13	C_14	C_15	C_16	Total	U_Accuracy	Kappa
	0	C_1	9	0	0	0	0	0	0	0	0	0	0	0	9	1	0
	1	C_2	0	0	0	0	0	0	1	0	0	0	0	0	1	0	0
	2	C_3	0	1	4	0	7	0	0	0	0	0	0	0	12	0.333333	0
	3	C_4	0	0	0	1	0	0	0	0	0	0	0	0	1	1	0
	4	C_5	0	3	7	0	53	4	1	0	0	0	0	0	68	0.779412	0
	5	C_10	0	0	0	0	0	0	1	0	0	0	0	0	1	0	0
	6	C_11	0	0	0	0	0	1	3	0	0	0	0	0	4	0.75	0
	7	C_12	1	0	0	8	0	0	0	9	1	0	2	5	26	0.346154	0
	8	C_13	0	6	0	1	6	0	2	1	10	0	0	3	29	0.344828	0
	9	C_14	0	0	0	0	0	5	2	0	0	10	0	0	17	0.588235	0
	10	C_15	0	0	0	0	0	0	0	0	0	0	8	0	8	1	0
	11	C_16	0	0	0	0	0	0	0	0	0	0	0	2	2	1	0
	12	Total	10	10	11	10	66	10	10	10	11	10	10	10	178	0	0
	13	P_Accuracy	0.9	0	0.363636	0.1	0.80303	0	0.3	0.9	0.909091	1	0.8	0.2	0	0.61236	0
	14	Kappa	0	0	0	0	0	0	0	0	0	0	0	0	0	0.528613	0

Figure 13: Confusion matrix generated from false color band combination classification

Table																	
<div><div><div></div><div></div><div></div><div></div><div></div><div></div></div><div><div></div><div></div><div></div><div></div><div></div><div></div></div><div><div></div><div></div><div></div><div></div><div></div><div></div></div><div><div></div><div></div><div></div><div></div><div></div><div></div></div><div><div></div><div></div><div></div><div></div><div></div><div></div></div><div><div></div><div></div><div></div><div></div><div></div><div></div></div></div>																	
VEGETATION_CONFUSE																	
	OID	ClassValue	C_1	C_2	C_3	C_4	C_5	C_10	C_11	C_12	C_13	C_14	C_15	C_16	Total	U_Accuracy	Kappa
▶	0	C_1	8	0	0	0	0	0	0	0	0	0	0	0	8	1	0
	1	C_2	0	1	0	0	0	0	0	0	0	0	0	0	1	1	0
	2	C_3	0	0	5	0	11	4	0	0	2	0	0	0	22	0.227273	0
	3	C_4	0	0	0	1	0	0	0	0	0	0	0	0	1	1	0
	4	C_5	0	1	5	0	44	1	0	0	1	0	0	0	52	0.846154	0
	5	C_10	0	0	0	0	0	0	0	0	0	0	0	0	0	0	0
	6	C_11	0	0	0	0	0	1	3	0	0	0	0	0	4	0.75	0
	7	C_12	1	0	0	7	0	0	0	8	1	0	2	2	21	0.380952	0
	8	C_13	0	8	1	2	11	1	4	2	7	0	0	3	39	0.179487	0
	9	C_14	0	0	0	0	0	3	3	0	0	10	0	0	16	0.625	0
	10	C_15	0	0	0	0	0	0	0	0	0	0	8	0	8	1	0
	11	C_16	1	0	0	0	0	0	0	0	0	0	0	5	6	0.833333	0
	12	Total	10	10	11	10	66	10	10	10	11	10	10	10	178	0	0
	13	P_Accuracy	0.8	0.1	0.454545	0.1	0.666667	0	0.3	0.8	0.636364	1	0.8	0.5	0	0.561798	0
	14	Kappa	0	0	0	0	0	0	0	0	0	0	0	0	0	0.48446	0

Figure 14: Confusion matrix generated from Vegetation band combination classification

ClassValue	Class_name
C_1	WATER
C_2	WATER
C_3	AIRPORT
C_4	GRASS
C_5	ATHLETIC FIELD
C_10	SAGEBRUSH
C_11	SOIL
C_12	URBAN
C_13	AGRICULTURAL
C_14	ROAD
C_15	SAND
C_16	FOREST

Figure 15: Legend land cover types for confusion matrix tables

The tables shown above summarize the relationship between the “ground truth” (columns) classified image and the classified image (rows). The U_Accuracy column represents the User’s accuracy and shows “pixels that are incorrectly classified as a known class when they should be classified as something else”. This error is also called an error of commission or type 1. The P_Accuracy row represents the producer’s accuracy and it indicates the number of “pixels of a known class that are classified as something other than that class”. This error is also called an error of commission or type-2. The Kappa index shown in the bottom right hand corner indicates the overall accuracy of the assessment.¹⁰ The three values described above range from zero to one with zero indicating no agreement and one indicating complete agreement. The diagonal line shown highlighted in figures 13 and 14 indicate the number of correctly identified pixels. It should be noted that the accuracy is only assessed for the pixel that is directly under the point that is randomly generated so more points would produce a more thorough assessment. Applying this knowledge to the classifications performed on the different band combination composite images reveals that both classifications exhibit moderate agreement with the ground truth image but that the false color classification was more accurate than the vegetation band combination classification when compared to the natural color band combination classification. The stark delineation of healthy vegetation is one of the primary visual benefits afforded by the false color infrared image which also supports the conclusion that it is a better band combination for land cover studies.

Conclusions

This project expanded upon the ideas and information presented during the lecture and afforded the opportunity to examine unfamiliar data products, image processing/ classification techniques, and accuracy assessment methods. The improvements Sentinel-2 data offer when compared to the Landsat missions quickly became apparent when the datasets were initially examined. The enhanced spectral and spatial resolutions of Sentinel-2 data provide an opportunity to increase the quality of land cover classification studies with no increase in cost or technical difficulty. The problems encountered with the European Space Agency STEP software that necessitated using QGIS for the atmospheric correction are not insurmountable and it is felt that using a software more closely coupled with the image producer would be advantageous. The limitations of ArcGIS as an image processing platform became apparent when comparing it to the ENVI software package that the author has used before. These limitations are felt most strongly when trying to statistically examine the imagery as well as when analyzing the information outside of the confusion matrix. Efforts were made to create polygons from the classified rasters and apply zonal statistics to no avail. This project necessitated developing a workflow that maintained the fidelity of the data and capitalized on the strengths of separate software packages for image processing and classification.

All land use studies would benefit immeasurably from exhaustive ground truth reconnaissance and this project is no exception. The accuracy of this project could have been further increased by reducing the number of classes and better isolating the spectral signature of each class. Further work is required to fully exploit the information available through the Sentinel-2 program and this project served as an introduction to the data and processing environments available at this time. I greatly look forward to the remote sensing class next semester and perhaps I can use these results as a baseline to work from and improve upon.

Bibliography

1. *Sentinel 2- Earth Resources and Science (EROS) Center*. U.S Department of the interior. May 21, 2018, Accessed Nov. 27, 2018. <https://eros.usgs.gov/remote-sensing/sentinel-2>
2. *ESA Sentinel online- processing levels*. European Space Agency. 2018. Accessed Nov. 27, 2018. <https://earth.esa.int/web/sentinel/user-guides/sentinel-2-msi/processing-levels/level-1>
3. *Sentinel-2 Products Specification Document*. European Space Agency. November 18, 2015. PDF
4. Tianxiang Zhang, et al. *Band Selection in Sentinel-2 Satellite for Agriculture Applications*. 2017. PDF
5. *LandSAT 8 Data Users Handbook- Section 2*. U.S. Department of the Interior. October 18, 2018. Accessed Nov. 27, 2018. <https://landsat.usgs.gov/landsat-8-l8-data-users-handbook-section-2>
5. Congedo, Luca. *Semi-Automatic Classification Plugin Documentation*. June 13, 2018. PDF
6. *ESA Sentinel online- processing levels*. European Space Agency. 2018. Accessed Nov. 27, 2018. <https://sentinel.esa.int/web/sentinel/user-guides/sentinel-2-msi/processing-levels/level-2>
7. *Geospatial Training and Applications for Ethiopia*. Colorado State University. Fort Collins. 2018. PDF https://ethiopia-gis.nrel.colostate.edu/pdf/RSLessons/RS_Lesson_2_Image_Interpretation.pdf
8. Adams, John & Gillespie, Allan. *Remote Sensing of Landscapes with Spectral Images*. Cambridge University Press. 2006.
9. *How Maximum Likelihood Classification Works- ArcGIS Help*. ESRI. 2018. Accessed Nov. 27, 2018. <http://desktop.arcgis.com/en/arcmap/latest/tools/spatial-analyst-toolbox/how-maximum-likelihood-classification-works.htm>
10. *Compute Confusion Matrix- ArcGIS Help*. ESRI. 2018. Accessed Nov. 27, 2018. <http://desktop.arcgis.com/en/arcmap/latest/tools/spatial-analyst-toolbox/compute-confusion-matrix.htm>